

Analysis of the energy distributions of escaping suprathermal ions in the TJ-II by means of a flexible luminescent probe with energy and pulse resolution

M. Martínez¹, B. Zurro², A. Baciero², D. Jiménez-Rey², V. Tribaldos³ and TJ-II Team

¹*Universidad Carlos III de Madrid, Leganés, Spain.*

²*Laboratorio Nacional de Fusión, CIEMAT, Avenida Complutense 40, 28040 Madrid, Spain*

³*Departamento de Física, Universidad Carlos III de Madrid, Leganés, Spain*

INTRODUCTION. The existence of a significant population of suprathermal ions in TJ-II stellarator plasmas heated by ECRH has been demonstrated previously by passive spectroscopy [1] and luminescent probe (LP) data [2]. In addition, the LP was configured to detect individual ions with time and energy resolution [3] and has been used to perform an overall view of suprathermal ions in ECRH and NBI phases of the TJ-II stellarator and its relation with spectroscopic observations [4]. In a previous work, the suprathermal temperature (T_{sp}) exhibits a rise and fall time as fast as thermal T_e , when a modulation of gyrotrons is used. This feature suggests that the suprathermal ions are directly related to the ECRH power (P_{ECRH}) and not to an intermediate heating by neither thermal electrons nor suprathermal electrons [5]. The pulse operational mode of the ion detector is directly related to velocity distribution function[6] of the measured particles by

$$J(W, \alpha, x) = \frac{2W}{m^2} f(W, \alpha, x)$$

where $J(W, \alpha, x)$ is the differential particle flux, per unit area at a given energy (W), pitch angle (α), position (x) and f is the distribution. This work is focused on the study of the ion energy distribution functions under different TJ-II plasma conditions: effects of real time scanning the magnetic configuration, on-axis vs off-axis ECRH heating and discharges with different density and different level of P_{ECRH} .

EXPERIMENT. TJ-II is a four-period, low magnetic shear stellarator with major and averaged minor radii of 1.5 m and ≤ 0.22 m, respectively. Central electron densities and temperatures up to $1.7 \times 10^{19} \text{ m}^{-3}$ and 1 keV respectively are achieved for plasmas created and maintained by ECRH at the second harmonic ($f = 53.2 \text{ GHz}$, $P_{ECRH} \leq 500 \text{ kW}$). Both gyrotrons were focused either on-axis or off-axis (effective minor radius $r/a \approx 0$ or $r/a \approx 0.33$, respectively). The LP used has been previously reported [2] and the luminescent screen used

in this experiment was made of TG-Green (decay time of 500 ns).

RESULTS. In Fig. 1, the density evolution of the selected discharges studied in this work are depicted; number of discharge, power, type of ECRH heating (on, off) and rotational transform ($\iota/2\pi$) at the center are given in the accompanying frame. In Figure 2(a) shows the change in suprathermal ion temperature, T_{sp} , for a discharge (#35992) where the magnetic configuration was scan during the discharge, in comparison with a reference discharge (#35991), whose configuration was fix. In Figure 2(b) we compare T_{sp} for two similar discharges heated by on (#34996) and off (#32741) axis gyrotrons.

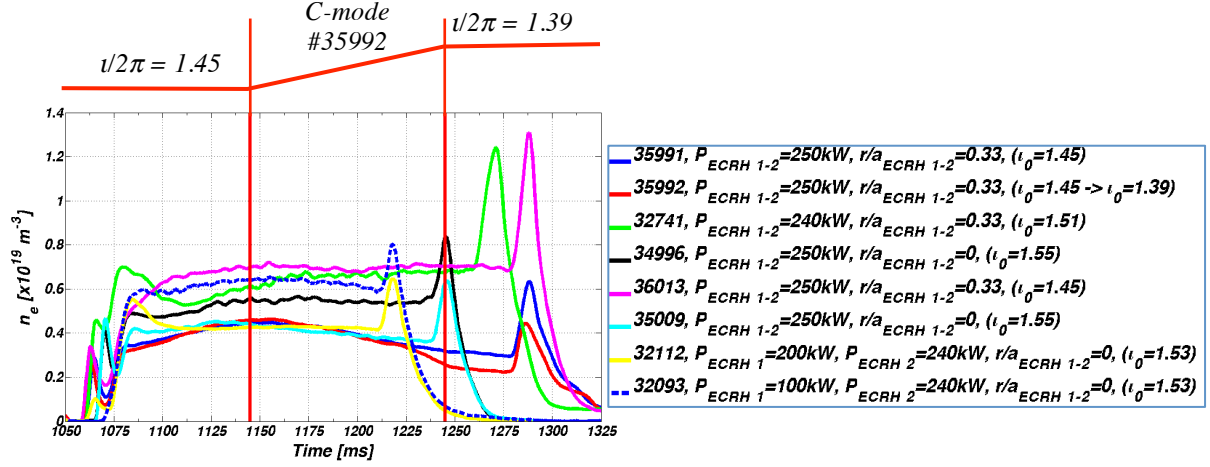


Figure 1. Density evolution for different discharges. Different values set up are sketched. Also, it shows the times for the magnetic configuration change (1145 ms – 1245 ms) for # 35992.

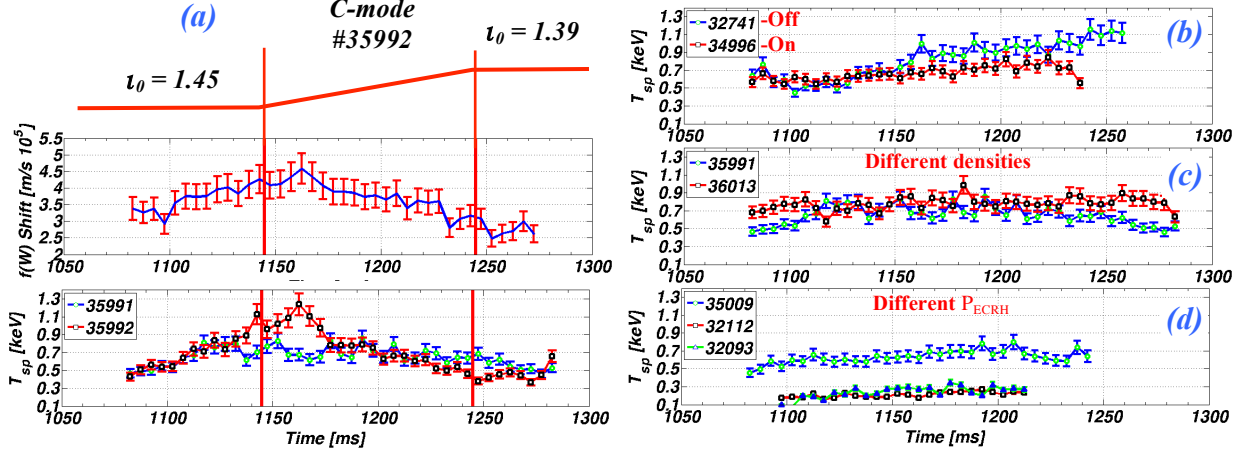


Figure 2. T_{sp} Evolution for several discharges (a) case of a magnetic configuration scan; distribution shift is shown at the top; (b) effect of off-axis (# 32741) and on-axis (# 34996) heating; (c) discharges with the same set up, but different densities ($\langle n_e \rangle_{36013} = 0.69$ and $\langle n_e \rangle_{35991} = 0.39$, in flat top); and (d) discharges with different P_{ECRH} (#35009, #32112 and #32093, where P_{ECRH} are 250 kW, 200 kW and 100 kW, respectively).

From suprathermal ion distribution functions its temperature, T_{sp} , were calculated, see Figure 2. The #35991 (fixed magnetic configuration) shows two components (see Figure 3). This double distribution is observed throughout the evolution of the discharge. However, for discharge #35992, the double distribution disappears in the ramp sweep but reappears once it

reaches the next stable magnetic configuration. It is also shown that the maximum of the ion distribution has a shift during the ramp sweep, changing the first distribution tail and making impossible to distinguish the two distributions observed in the stable configurations. The T_{sp} of #34996 (on-axis) is higher than T_{sp} #32741 (off-axis) and distributions are best defined in the former than in the later one (see Figure 4). In discharges #35991 and #36013, with different plasma densities, the same trend in T_{sp} is observed. But in discharge #36013 (with higher density), T_{sp} tends to be higher than in the second distribution of #36013 (see Figure 5(a)).

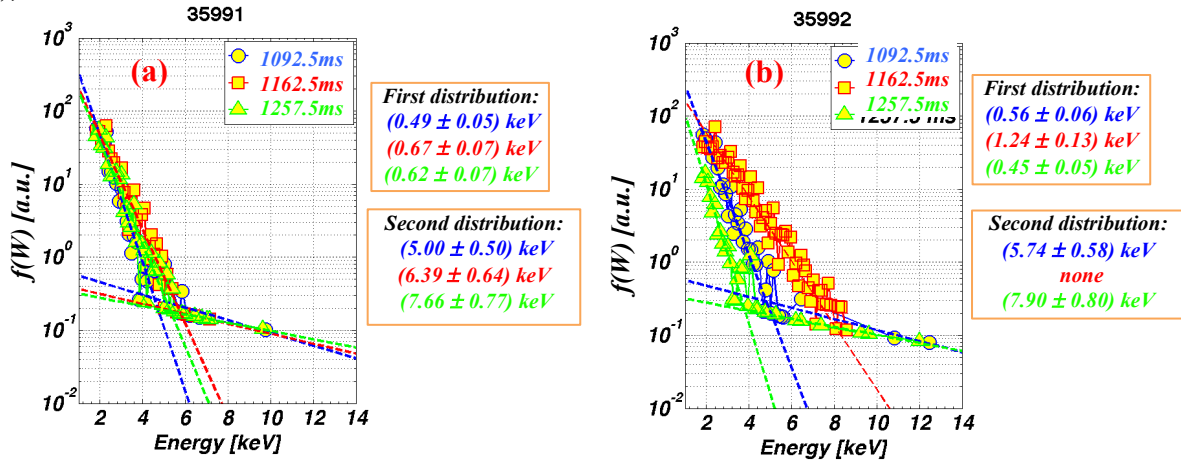


Figure 3. (a) Discharge #35991 ($\nu/2\pi = 1.45$) shows two suprathermal ion distributions along the discharge evolution, (b) Discharge #35992 (scanning from $\nu/2\pi = 1.45 \rightarrow \nu/2\pi = 1.39$) shows two distributions at the beginning and at the end of the discharge. But the second distribution disappears while scanning the magnetic configuration.

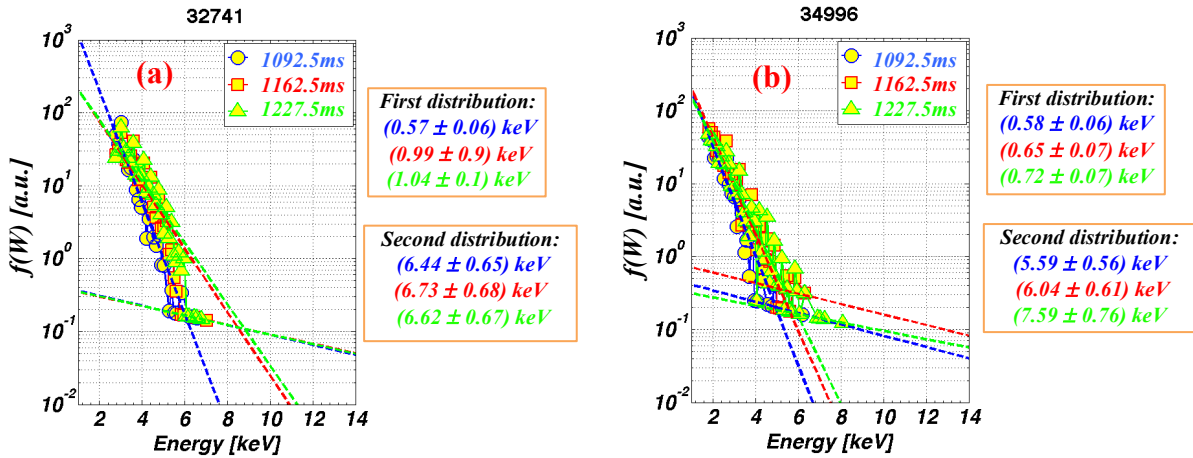


Figure 4. Suprathermal ions distributions are shown in ECRH set up (a) off-axis and (b) on-axis.

The difference between shots #35009 and #32112 is very evident in the values of T_{sp} (see Fig. 2(d)) and it can be understand by the distribution functions depicted in Figures 5(b) and 5(c). For the #35009, P_{ECRH} is enough to generate suprathermal ions with wider distributions and even it generates a second distribution of them. But in #32112 there was not enough power to generate a second distribution, while the main distribution is very narrow (see Figure 5(c)).

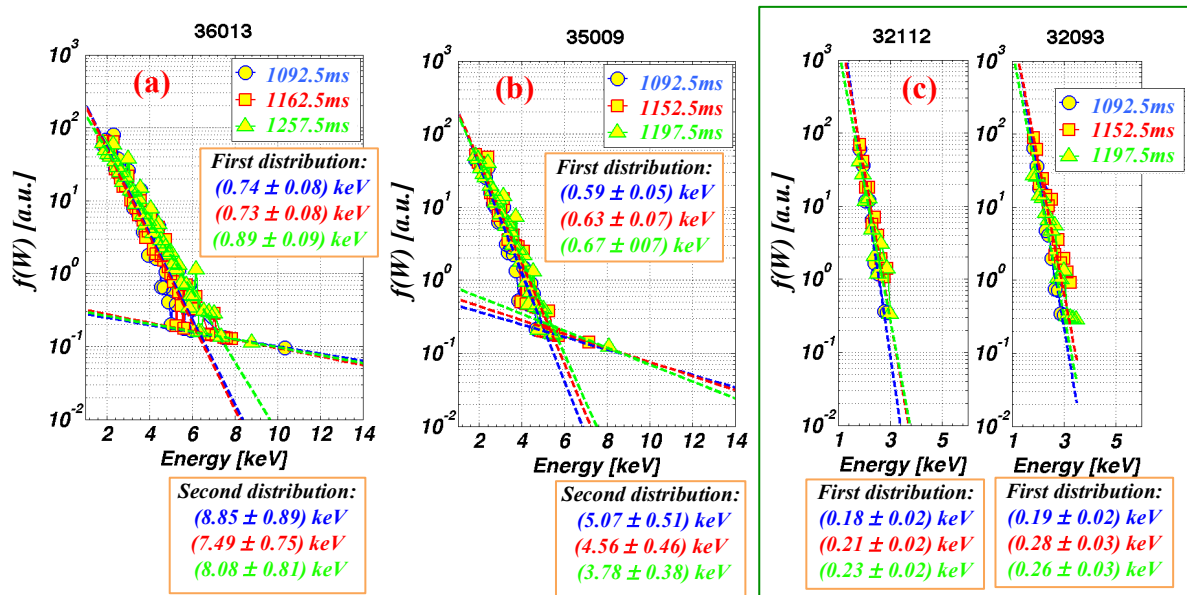


Figure 5. (a) #36013, discharge with the same set up of #35991 but with higher plasma density (see Figure 1). (b) #35009 and (c) #32112 - #32093 (green square) have similar set up but with different P_{ECRH} (250 kW, 200 kW and 100 kW, respectively).

In conclusion, it has been shown the time behaviour of the suprathermal ion population generated by the ECRH in TJ-II and measured by a luminescent probe operating in the ion counting mode with energy discrimination [3]. Apart from the distribution simultaneous to the RF heating previously studied [5], we present here evidence that there is a second distribution of suprathermal ions, which remains constant over discharge time. This second distribution can be smeared out by magnetic configuration scanning, which modify the distribution and makes wider its tail, or even does not appear if there is not enough ECRH power. It has been also shown that the increase in n_e does not significantly affect the energy of the suprathermal ions (see Figures 3(a) and 5(a)), or the temperature of the main distribution, but it does affect the second distribution of the ions. The influence of on-axis or off-axis heatings on the suprathermal ion distributions was reported being T_{sp} higher when the ECRH is off-axis.

ACKNOWLEDGEMENTS. This work was partially funded by the Spanish “Ministerio de Economía y Competitividad” under Grant No. ENE2010-19109. One of the authors (M. M.) would like to thank CONACYT (Mexico) for his scholarship.

REFERENCES

- [1] D. Rapisarda, B. Zurro, V. Tribaldos, A. Baciero, et al., *Plasma Phys. Control. Fusion* **49**, 309 (2007).
- [2] D. Jiménez-Rey, B. Zurro, J. Guasp et al., *Rev. Sci. Instrum.* **79**, 093511 (2008).
- [3] B. Zurro, A. Baciero et al., *Rev. Sci. Instrum.* **83**, 10D306 (2012).
- [4] B. Zurro, A. Baciero, V. Tribaldos et al. *Nuclear Fusion* **53**, 083017 (2013).
- [5] B. Zurro, A. Baciero et al., 40th EPS Conference on Plasma Physics, Proceedings: ocs.ciemat.es/EPS2013PAP/pdf/P4.177.pdf
- [6] W. Baumjohann, R. A. Treumann, *Basic Space Plasma Physics*, Imperial College Press (1992).